

Photon rings and shadows of Kerr black holes immersed in a swirling universe

Rogério Capobianco*

Instituto de Física de São Carlos, Universidade de São Paulo, São Carlos, São Paulo 13560-970, Brazil &

Institut für Physik, Carl-von-Ossietzky Universität Oldenburg, 26111 Oldenburg, Germany

Betti Hartmann† and Nikhita Vas‡

Department of Mathematics, University College London, Gower Street, London, WC1E 6BT, UK

Jutta Kunz§

Institut für Physik, Carl-von-Ossietzky Universität Oldenburg, 26111 Oldenburg, Germany

(Dated: October 3, 2025)

We discuss photon rings around as well as shadows of Kerr black holes immersed in a swirling spacetime. We find that the spin-spin interaction between the angular momentum of the black hole and the swirling of the background leads to new interesting effects as it breaks the symmetry between the upper and lower hemispheres. One of the new features of the spin-spin interaction is the existence of up to three light rings for suitable choices of the angular momentum parameter a and swirling parameter j . In comparison to the Schwarzschild black hole immersed in a swirling universe, the light rings typically all possess different radii.

1. INTRODUCTION

Obtaining exact solutions to the Einstein equation is no easy task. Such solutions can only be found once symmetries are imposed. Exact solutions of the Einstein equation are of particular importance, since these allow us to study the effects of gravity using analytical techniques. Rotation is a characteristic observed in all celestial objects in our universe, and the Kerr spacetime is an exact solution representing a stationary rotating black hole (BH). Other exact, rotating solutions are, for instance, the Gödel Universe [1], where homogeneous dust is rotating around every point, or the Taub-NUT solution [2, 3], where the NUT charge gives a rotational sense to the spacetime.

Recently, a new exact, rotating solution has been constructed using the Ernst formalism [4]. This solution describes a rotating Kerr black hole in a swirling universe [5]. The swirling universe, i.e. the solution without the black hole, is a vacuum solution equipped with an odd- \mathbb{Z}_2 symmetry: the upper ($\theta \in [0 : \pi/2]$) and lower hemispheres ($\theta \in [\pi/2 : \pi]$) of the spacetime rotate in opposite directions. The swirling universe can, in fact, be obtained by using the Lie point symmetry through the application of the Ehlers transformation. Note that the geodesic motion can be decoupled and completely integrated in this spacetime [6]. An interesting question is whether this solution is of potential observational relevance, and which new features appear that allow distinction from the “pure” Kerr spacetime. An analysis of accretion discs in this spacetime has already been performed, revealing their bowl-like structure [7]. Recently, the interest in generating techniques has grown again, and different new solutions including the swirling background have been constructed. In particular, external electromagnetic fields were considered in a composition of Harrison and Ehlers’ transformation [8], as well as charged black holes, i.e. Kerr-Newman black holes immersed in the swirling background [9, 10].

In this work we aim to contribute to the exploration of the phenomenological imprints of black holes immersed in the swirling universe. A main objective of this paper is to study the existence and location of circular photon orbits, also known as *light rings* (LRs), in the spacetime of a Kerr black hole immersed in a swirling universe (KBHSU). The motion of light-like particles is one of the main probes of a curved spacetime. Furthermore, null geodesics can be used to study gravitational waves at very large angular momenta, i.e. in the so-called eikonal limit, and a link between quasi-normal mode frequencies and unstable light rings can be drawn [11]. Furthermore, all BHs formed from stellar collapse, that is, stationary, axially symmetric, and asymptotically flat solutions in 3 + 1 dimensions with a non-extremal, topologically spherical Killing horizon must possess at least one circular photon orbit outside the horizon, thus LRs are present in many black hole spacetimes, such as the Schwarzschild, Reissner-Nordström, Kerr,

* rogerio.capobianco@gmail.com

† b.hartmann@ucl.ac.uk

‡ nikhita.vas.18@ucl.ac.uk

§ jutta.kunz@uni-oldenburg.de

and Kerr-Newman spacetimes [12], as well as in spacetimes of other objects, that are dubbed ultracompact objects (UCOs) precisely because they feature LRs [13–15].

The LRs of Schwarzschild black holes in a swirling universe (SBHSU) have previously been investigated in [16]. Because of the swirling motion, the degenerate light ring of the Schwarzschild black hole splits into two LRs that are located symmetrically in planes above and below the equatorial plane. Whereas the LRs counter-rotate with respect to each other, each of them co-rotates with respect to the swirling background universe. Here we investigate how the additional angular momentum of the Kerr black hole affects the location, the rotational sense, and the number of LRs.

A related objective is the calculation of the shadows of the Kerr black holes in a swirling universe. While there has been work on photon spheres and shadows of rotating black holes for decades (see e.g. [17–20]), it is the observations of M87* and Sgr A* by the EHT collaboration [21, 22] that make the study of shadows most relevant. Recently, the shadow of a SBHSU has been investigated in [16], revealing the interesting new feature, that the shadow became twisted, i.e., it inherited the odd- \mathbb{Z}_2 symmetry of the swirling universe with respect to the equatorial plane. This symmetry is broken by the spin of the Kerr black hole. Here, we investigate how this affects the shadow.

We also address further properties of the KBHSU spacetime such as its conical singularities and its ergoregions. Our studies show that the value $ajM = 0.25$, i.e. the combination of the swirling parameter j , the (seed) angular momentum parameter a , and the mass parameter M of the seed Kerr black hole, is a critical value for the properties of the spacetime.

This manuscript is organised as follows: in section 2, we recall the metric of the KBHSU spacetime, derive the conical singularities, and determine the ergoregions. In section 3, we address the motion of light-like particles, evaluate the LRs and determine their dependence on the parameters j and a of the spacetime. We obtain the shadows in section 4, and conclude in section 5.

We have adopted geometrized units, i.e., $G = c = 1$. The swirling parameter has dimensions of $[j] = M^{-2}$. We will choose $M = 1$ in the following, unless otherwise stated.

2. THE SPACETIME AND ITS PROPERTIES

The metric tensor describing the KBHSU can be generated by applying an Ehlers transformation on a Kerr black hole seed solution within the Ernst formalism [4]. In Boyer-Lindquist coordinates, it reads [4] :

$$ds^2 = \frac{1}{\mathcal{F}(r, \theta)} (d\varphi - \omega dt)^2 + \mathcal{F}(r, \theta) \left[-\rho^2 dt^2 + \Sigma \sin^2 \theta \left(\frac{dr^2}{\Delta} + d\theta^2 \right) \right], \quad (1)$$

where the functions \mathcal{F} and ω are expressed as a second-order series in the swirling parameter j as follows :

$$\mathcal{F} = \frac{\mathcal{F}_0 + j\mathcal{F}_1 + j^2\mathcal{F}_2}{R^2 \Sigma \sin^2 \theta} \quad , \quad \omega = \frac{\omega_0 + j\omega_1 + j^2\omega_2}{\Sigma} \quad , \quad (2)$$

with

$$\begin{aligned} \mathcal{F}_0 &= R^4, & \mathcal{F}_1 &= 4aM\Xi \cos \theta R^2, & \mathcal{F}_2 &= 4a^2 M^2 \Xi^2 \cos^2 \theta + \Sigma^2 \sin^4 \theta \\ \omega_0 &= 2aMr, & \omega_1 &= 4 \cos \theta (Ma^4 - r^4(r - 2M) - \Delta a^2 r - a(r - M)\mathcal{W}), \\ \omega_2 &= 2M [3ar^5 - a^5(r + 2M) + 2a^3r^2(r + 3M) - r^3(\cos^2 \theta - 6)\mathcal{W} + a^2\mathcal{W}(\cos^2 \theta(3r - 2M) - 6(r - M))], \end{aligned}$$

and abbreviations

$$\begin{aligned} \Delta &= r^2 - 2Mr + a^2, & \rho^2 &= \Delta \sin^2 \theta, & \Sigma &= (r^2 + a^2)^2 - \Delta a^2 \sin^2 \theta, \\ \mathcal{W} &= \Delta a \cos^2 \theta, & \Xi &= r^2 (\cos^2 \theta - 3) - a^2 (1 + \cos^2 \theta), & R^2 &= r^2 + a^2 \cos^2 \theta. \end{aligned}$$

Here, the quantities M and $a = J/M$ are inherited from the Kerr seed solution¹. We will refer to these parameters as “the mass parameter” and “the angular momentum parameter” in the following, respectively. For $j = 0$ the above

¹ Note that J is the seed black hole’s total angular momentum that has no link to the swirling parameter.

metric describes the Kerr spacetime, while for $a = 0$ the line element corresponds to that of a Schwarzschild black hole in a swirling universe. When the quantities originating from the black hole vanish, i.e., for $a = M = 0$, we recover the pure swirling background.

The compact object still possesses two horizons which, in these coordinates, are obtained by $\Delta = 0$, i.e., $r_h^{(\pm)} = M \pm \sqrt{M^2 - a^2}$. Note that, although the locations of the horizons are independent of j and mapped on the same surfaces as the Kerr seed solution, the geometry of the horizons when considering an isometric embedding deforms the horizon shape due to the background's frame dragging. However, despite the modifications in the event horizons' shape, the area remains unaffected [7].

2.1. Conical singularity

The spacetime is non-asymptotically flat and has a non-removable conical singularity. We can identify the existence of an axial angular deficit/excess by considering the ratio between the perimeter and radius of a small circle around the rotational axis at both the north and the south poles [4, 9, 10]

$$\delta_0 = \lim_{\theta \rightarrow 0} \frac{1}{\theta} \int_0^{2\pi} \sqrt{\frac{g_{\varphi\varphi}}{g_{\theta\theta}}} d\varphi \quad \text{and} \quad \delta_\pi = \lim_{\theta \rightarrow \pi} \frac{1}{\pi - \theta} \int_0^{2\pi} \sqrt{\frac{g_{\varphi\varphi}}{g_{\theta\theta}}} d\varphi. \quad (3)$$

If $\delta_0 = \delta_\pi = 2\pi$, then there is no conical singularity. In the KBHSU spacetime, however, we have [4]

$$\delta_0 = \frac{2\pi}{(1 - 4ajM)^2} \quad \text{and} \quad \delta_\pi = \frac{2\pi}{(1 + 4ajM)^2}, \quad (4)$$

for non-vanishing angular momentum parameter a and finite j . Thus the SBHSU does not suffer from conical singularities. We note the divergence for the critical value $ajM = \pm 0.25$.

2.2. Ergoregions

A typical characteristic observed in the swirling family of solutions is the appearance of non-compact ergoregions extending from the equatorial plane to infinity [4, 7, 9, 10]. An ergoregion is defined by $g_{tt} > 0$ with boundary at $g_{tt} = 0$. For the KBHSU spacetime this reads $\omega^2/\mathcal{F} - \rho^2\mathcal{F} > 0$ with boundary at $\omega^2 = \rho^2\mathcal{F}^2$. The angular velocity Ω of the frame dragging is given by $\Omega = -g_{t\varphi}/g_{\varphi\varphi} = \omega$, which is not constant. We focus our analysis on the region outside the event horizon. The cross section of the ergoregions with the plane $y = 0$ ($\varphi = 0, \pi$) and their frame dragging directions are shown in Fig. 1 for two values of the angular momentum parameter, $a = 0.1M$ and $a = 0.8M$, and several values of jM^2 , excluding the region behind the event horizon. For sufficiently small j , we observe three disconnected surfaces: one compact region inherited from the black hole which encompasses the horizon, and two non-compact regions which extend to spatial infinity above and below the equatorial plane. The latter are already present in the swirling universe [4, 6]. The ergoregion in the upper hemisphere counter-rotates with respect to the black hole's spin, i.e., $\Omega < 0$ (coloured red), while the one in the lower hemisphere co-rotates with $\Omega > 0$ (coloured blue). Note that the ergoregion inherited from the Kerr spacetime around the event horizon is always present for a finite value of the angular momentum parameter, but only becomes visible in the plots for large enough a (see Fig. 1b).

Similar to the SBHSU [16], we find that by increasing j , the boundaries of both the upper and lower ergoregions move closer to the horizon. However, whilst in the $a = 0$ case they never interfere with the horizon, for $a \neq 0$ and sufficiently large j , the two disconnected patches below and above the equatorial plane merge with the ergoregion surrounding the horizon. For a positive swirling parameter and increasing j , the lower ergoregion with $\Omega > 0$ joins the black hole's ergosphere first. Once j reaches the critical value such that $ajM = 0.25$, the upper patch joins the merged region to form an infinitely extended ergoregion that surrounds the horizon. This single ergoregion now has angular velocity $\Omega > 0$ everywhere and possesses a cylindrical shape. For very small a and large j the ergoregion shrinks to very small width.

In summary, the structure of the ergoregions for small j appears similar to that of the SBHSU case [16], but differs significantly when j increases. In the SBHSU, there is always symmetry about the equatorial plane. However, when a increases, the spin-spin interaction starts to play a crucial role in the geometry of the ergoregions. The symmetry about the equatorial plane is broken, and the ergoregions eventually merge, forming a single region that extends all the way to infinity.

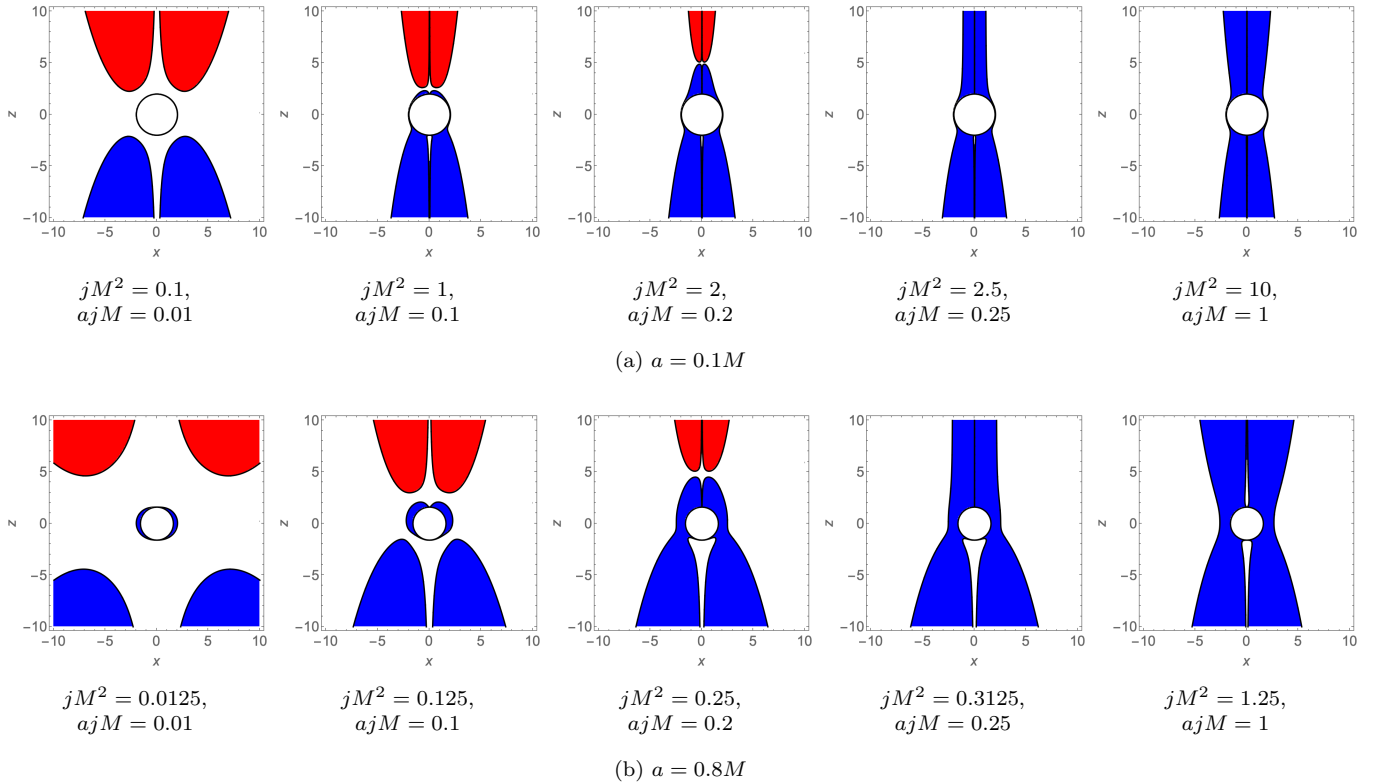


Fig. 1: Cross section ($x = r \sin \theta \cos \varphi$, $y = r \sin \theta \sin \varphi$, $z = r \cos \theta$, with $\varphi = 0, \pi$) of the ergoregions (coloured) with different values of jM^2 and (a) $a = 0.1M$ and (b) $a = 0.8M$. The angular velocity of frame dragging $\Omega = \omega$ in these regions is positive when coloured blue and negative when coloured red. The region behind the event horizon $r < r_h^{(+)}$ has been excluded from these plots.

3. PHOTON ORBITS

In this section, we discuss how light-like particles move on geodesics in the KBHSU spacetime. We employ the Hamiltonian formulation with

$$\mathcal{H} = \frac{1}{2}g^{\mu\nu}p_\mu p_\nu = 0, \quad (5)$$

where $p_\mu \equiv g_{\mu\nu}\dot{x}^\nu$ is the photon's 4-momentum. Then the respective Hamilton's equations read

$$\dot{x}^\mu = \frac{\partial \mathcal{H}}{\partial p_\mu}, \quad \dot{p}^\mu = -\frac{\partial \mathcal{H}}{\partial x_\mu}. \quad (6)$$

The spacetime admits two constants of motion owing to the geometry's stationarity and axisymmetry, which give rise to the Killing vector fields ∂_t and ∂_φ , respectively. Such fields entail two quantities that are conserved along the geodesics, related to the particle's four-momentum:

$$p_t = g_{tt}\dot{t} + g_{t\varphi}\dot{\varphi} = -E \quad \text{and} \quad p_\varphi = g_{\varphi\varphi}\dot{\varphi} + g_{t\varphi}\dot{t} = L, \quad (7)$$

where E and L are usually referred to as the energy and angular momentum of the particle, respectively. Solving the system (7) for the velocities and inserting the metric (1), one finds

$$\dot{t} = \frac{E - \omega L}{\mathcal{F}\rho^2}, \quad \dot{\varphi} = \mathcal{F}L + \frac{\omega(E - \omega L)}{\mathcal{F}\rho^2}. \quad (8)$$

Additionally, the normalization condition becomes

$$\Sigma \sin^2 \theta (\dot{r}^2 + \Delta \dot{\theta}^2) = \Delta \left(-L^2 + \frac{(E - \omega L)^2}{\mathcal{F}^2 \rho^2} \right). \quad (9)$$

In contrast to the Kerr spacetime, the r - and θ -motion is not separable in the KBHSU spacetime, i.e., no equivalent of the Carter constant exists. The spacetime is algebraically general, that is, Petrov type I [4].

3.1. Light rings

Light can travel on special circular paths, light rings (LRs), in the close vicinity of compact objects. A Schwarzschild black hole with mass parameter M has an unstable and planar LR at $r_p = 3M$. Due to the $SO(3)$ symmetry of the event horizon, $r_p = 3M$ then corresponds to the radius of the photon sphere surrounding the Schwarzschild black hole. Furthermore, a Kerr black hole possesses two LRs that are also located on the equatorial plane and are both unstable. The prograde ring has a radius that decreases from $3M$ to M as the angular momentum parameter a increases from zero to M , the so-called *extremal case*, while the radius of the retrograde ring increases from $3M$ to $4M$.

In general, the location of the LRs can be determined by finding the critical points of the effective potential V , which for a stationary and axially symmetric solution depends exclusively on the metric tensor and conserved charges. The effective potential reads

$$V = -\frac{1}{D}(E^2 g_{\varphi\varphi} + 2ELg_{t\varphi} + L^2 g_{tt}) \quad , \quad D = g_{t\varphi}^2 - g_{tt}g_{\varphi\varphi} . \quad (10)$$

Following [14, 24], we write V in terms of a pair of more manageable potentials H_{\pm} which depend only on the spacetime geometry

$$V = -\frac{L^2}{D}g_{\varphi\varphi}(\sigma - H_+)(\sigma - H_-) \quad , \quad H_{\pm}(r, \theta) = \frac{-g_{t\varphi} \pm \sqrt{D}}{g_{\varphi\varphi}} , \quad (11)$$

where $\sigma \equiv E/L$ is the inverse impact parameter. In this formalism, LRs are found as solutions of $V = 0 = \nabla V$. This therefore implies that a critical point of $H_{\pm}(r, \theta)$ must correspond to the coordinates of a LR, i.e., a pair (r_{LR}, θ_{LR}) such that $\nabla H_{\pm} = 0$.

For the KBHSU, with the metric (1) the potentials take a particularly simple form:

$$H_{\pm}(r, \theta) = \omega \pm \mathcal{F}\rho . \quad (12)$$

In the SBHSU, there is one degenerate LR on the equatorial plane at $r = 3M$, when $j = 0$, since in that case there is no distinction between co- and counter-rotation with respect to the swirling of the spacetime. However, as j increases, the degeneracy is broken and the LRs branch off: one into the upper hemisphere and one into the lower as seen in Fig. 2a. This pair of LRs is pushed off the equatorial plane and at the same time pulled towards the horizon. Note, in particular, that both LRs have the same radius. As $j \rightarrow \infty$, the LRs eventually reach the horizon $r = 2M$, with one LR at the North pole $\theta = 0$ and the other at the South pole $\theta = \pi$. In fact, for the SBHSU there is a symmetry of the effective potential such that if (r, θ) is a critical point of H_+ (shown in blue), then $(r, \pi - \theta)$ is also a critical point of H_- (shown in orange) [16].

For the KBHSU where $a \neq 0$, this symmetry no longer holds, though for small a , we observe similar features as those appearing in the SBHSU case: the LRs are again pushed off the equatorial plane and pulled towards the horizon. They now, however, start from the two different branches of LR locations for vanishing j , since co- and counter-rotating rings no longer agree for Kerr black holes.

The spin-spin interaction of the KBHSU gives rise to an interesting new feature : the emergence of three coexisting LRs. We observe this effect for all the values of a that we have studied, as demonstrated in Figs. 2b, 2c, 2d, and 2e. As seen in the figures, the third LR appears at the critical value $ajM = 0.25$. The new LR is a critical point of H_- which emerges from the axis $\theta = 0$ at large r and is then pulled inward while moving slowly away from the close vicinity of the axis. Shortly after the appearance of the third LR, however, the LR corresponding to the critical point of H_+ disappears.

In Fig. 3, we show the ergoregions for $a = 0.5M$ and $a = 0.9M$ and different values of jM^2 in the (r, θ) -plane and include the locations of all of the LRs for the respective parameter sets as well as the ergoregions (highlighted in light blue). Here, we indicate whether the direction of rotation of the LR is prograde (blue) or retrograde (red) with respect to the angular momentum of the BH. To find the rotational direction of the photon rings, we consider the azimuthal rotation given by the quantity Φ which is defined as :

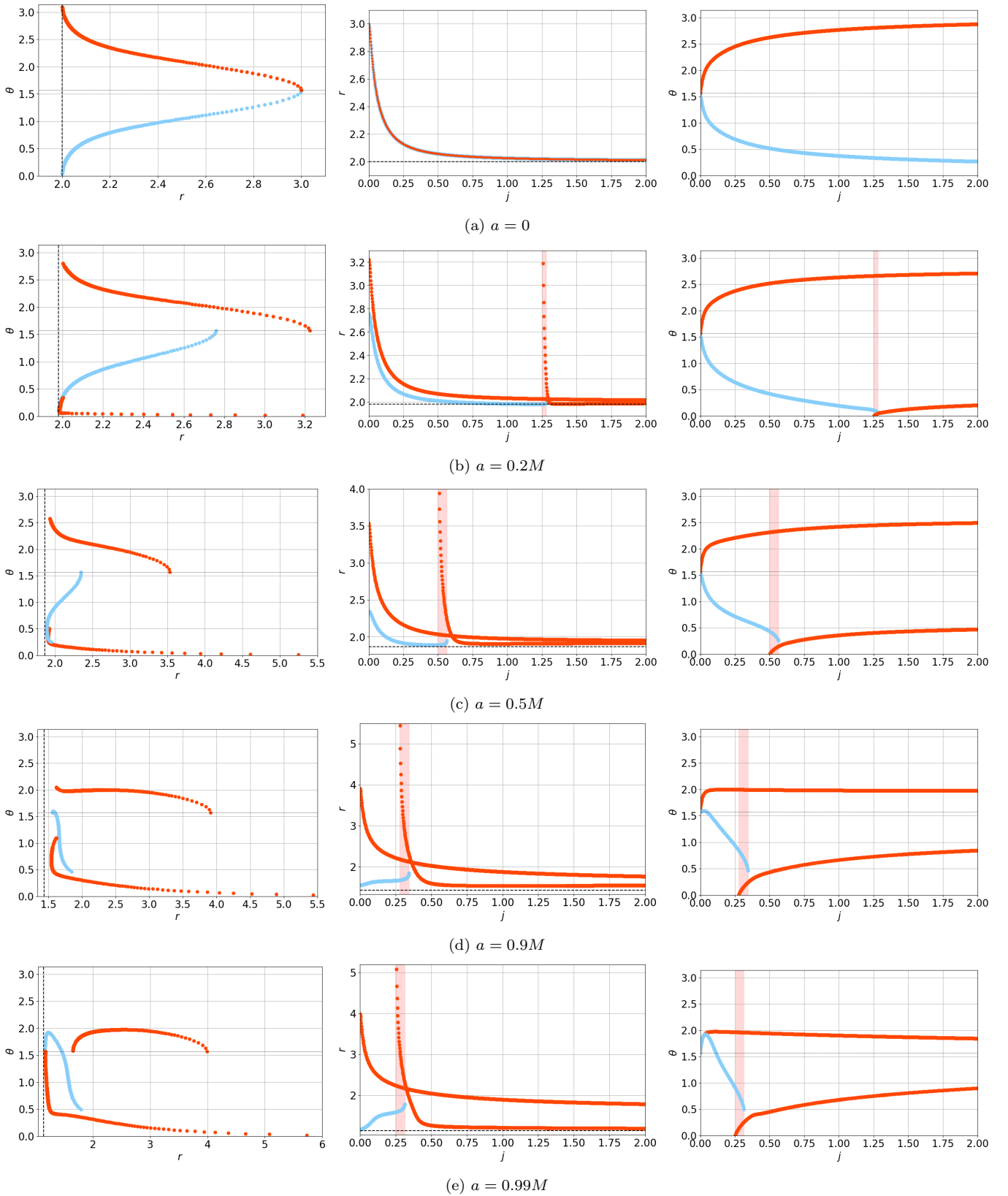


Fig. 2: Locations of LRs at multiples of $jM^2 = 0.002$ with $M = 1$. In the left-hand column we plot the coordinates of the LRs in the (r, θ) -plane, in the middle column we give the radial coordinate against j , and in the right-hand column we show the polar coordinate against j . LRs corresponding to H_+ are coloured blue, and LRs corresponding to H_- are in orange. The thick black dashed line represents the radius of the outer horizon. The pink vertical strip highlights the region where three LRs occur for the same value of j . The third LR appears around $ajM = 0.25$ and always begins at the North pole $\theta = 0$. The colours of the curves indicate whether the LR is a root of H_+ (light blue) or H_- (orange).

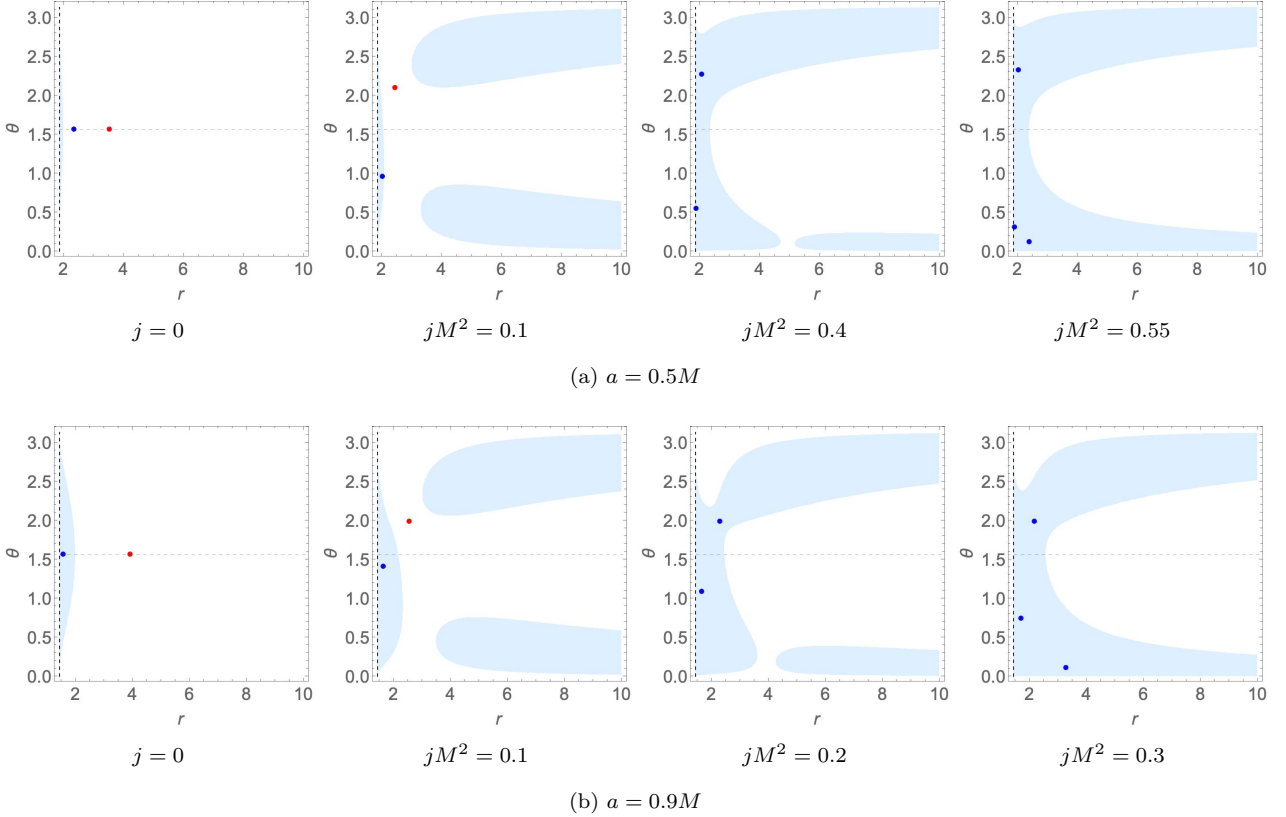


Fig. 3: Location of photon rings in the (r, θ) -plane for $a = 0.5M$ (upper row) and $a = 0.9M$ (lower row). The ergoregions are highlighted in light blue and the vertical dashed line represents the radius of the event horizon. The direction of rotation of the light rings is indicated by their colour : prograde orbits are represented by blue dots, while retrograde ones are represented by red dots. Note that prograde and retrograde here are with respect to the direction of the black hole rotation.

$$\Phi = \frac{d\varphi}{dt} = \frac{\dot{\varphi}}{t} = \frac{\mathcal{F}^2 \rho^2 L}{E - \omega L} + \omega. \quad (13)$$

In an asymptotically flat spacetime this would correspond to the rotational velocity with respect to a static asymptotic observer. At a light ring, we have the condition $V = 0$, i.e. $\mathcal{F}^2 \rho^2 L^2 = (E - \omega L)^2$, i.e., $E - \omega L = \pm \mathcal{F} \rho L$, hence we find

$$\Phi_{\pm} = H_{\pm} = \omega \pm \mathcal{F} \rho, \quad (14)$$

and thus the rotation of the LR associated with the H_+ depends on the sign of Φ_+ and the LR associated with the H_- depends on the sign of Φ_- . For the pure Kerr case, we always have two LRs on the equatorial plane: one retrograde orbit (red) and one prograde orbit (blue) which lies at a radius smaller than that of the retrograde orbit. This can be explained by the Lense-Thirring effect [19]. For sufficiently large BH angular momentum a , the prograde orbit lies inside the ergoregion (Fig. 3b). As j increases and the ergoregions expand, both LRs are pulled off the equatorial plane and eventually lie within the ergoregions, thus co-rotating with the swirling background.

4. SHADOWS

In this section, we will focus on the BH shadow and the lensing effect generated by the presence of the BH. The methods to study the shadow's silhouette depend on the integrability of the equations of motion. When the geodesic

motion for photons is separable, such as in the pure-Kerr case, the BH shadow can be obtained analytically [17]; for non-separable equations, a full numerical approach is required. Here, we follow the numerical method applied previously for the SBHSU solution [16]. Thus we apply a backwards ray-tracing method to integrate the equations of motion [24]. The geodesic equations for photons are then evolved backward in time starting from the *observer's* position. The photon's trajectory can either end by falling into the black hole, or once it reaches the *celestial sphere*. This is equivalent to considering light isotropically coming from every point in the celestial sphere and reaching the observer. A schematic representation is shown in Fig. 4.

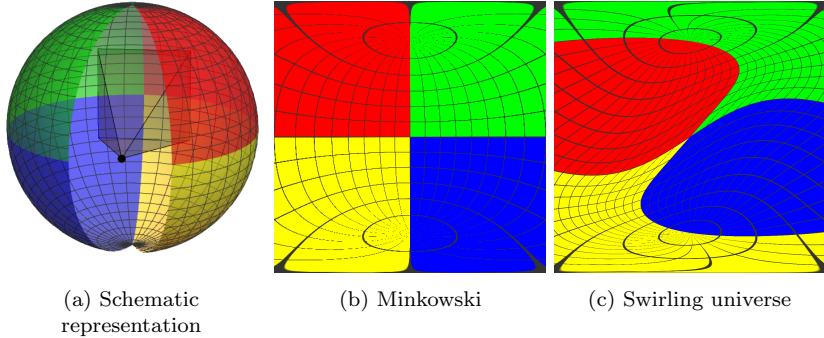


Fig. 4: (a) A schematic representation of the numerical setup. The small black sphere represents the observer, while the sphere with four coloured sections represents the celestial sphere (or the observer's sky). The observer's field of view is represented by a pentahedron in dark gray, resulting in the image seen by the observer. In (b), we show the view from a Minkowski spacetime, while in (c), the view is from a swirling universe with $j = 0.0005$.

The lensing images were produced using the PyHole package implemented in Python [24]. The observer is placed off-center at (r_o, θ_o) inside the celestial sphere, which is set to have a larger radius. The routine then integrates the equations of motion (6) using the Hamiltonian formalism with initial conditions set from the observer's position as follows :

$$p_r = \sqrt{g_{rr}} \cos \alpha \cos \beta , \quad (15)$$

$$p_\theta = \sqrt{g_{\theta\theta}} \sin \alpha , \quad (16)$$

$$p_\varphi = L = \sqrt{g_{\varphi\varphi}} \cos \alpha \sin \beta , \quad (17)$$

$$-p_t = E = \frac{1}{\sqrt{g_{\varphi\varphi}}} \left(\sqrt{D} - g_{t\varphi} \cos \alpha \sin \beta \right) , \quad (18)$$

where D was already defined in (10). To obtain an image, we scan over the observing angles (α, β) fixed by the observer's field of view. In our images, the celestial sphere is divided into four sections, each represented with a different colour. Overall, the black hole shadows present a clear asymmetrical pattern with the asymmetry more pronounced for an observer on the equatorial plane.

In the pure-Kerr case, since photons travelling in the direction of the frame dragging can orbit closer to the BH than photons travelling opposite to the frame dragging, this leads to a shadow that looks offset relative to the non-rotating case [25]. This effect is clearly observed for larger values of a . Once a non-zero value of the swirling parameter is considered, the shadow becomes *twisted*, as already observed in the Schwarzschild-swirling case [16]. To the first set of our images, we place the observer on the equatorial plane ($\theta_o = \pi/2$) at $r_o = 15$, and fixed the BH rotational parameter while the swirling parameter varies in the range $\{0, 10^{-3}\}$, those are shown in Fig. 5. Within the considered range of the swirling parameter, we see that the BH shadow becomes more prolate and twisted as j increases. We note, however, that the presence of both the angular momentum parameter a and the swirling parameter j breaks the odd \mathbb{Z}_2 symmetry present in the SBHSU case for observers in the equatorial plane. For non-equatorial observers, the spacetime asymmetry is less attenuated in our images. The images for an off-equatorial observer are shown in Fig. 6 for $a = 0.9M$, $j = 0.0008$, $r_o = 15$ and different values of θ_o .

Finally, we consider the effect of the Kerr rotational parameter a . To illustrate the effect, in Fig. 7 we show the shadows for black holes with different rotational parameters a while keeping the swirling parameter fixed at $j = 0.001$. Again, we have chosen $r_o = 15$ and $\theta_o = \pi/2$. As the value of a increases, the shadow becomes more asymmetric, already seen in the pure Kerr case, stands still once the swirling background is considered; this effect is attenuated

for slowly rotating BHs and thus is easily visualized for rapidly rotating compact objects. To demonstrate this, we show the lensing effect of a BH approaching extremality in Fig. 7c.

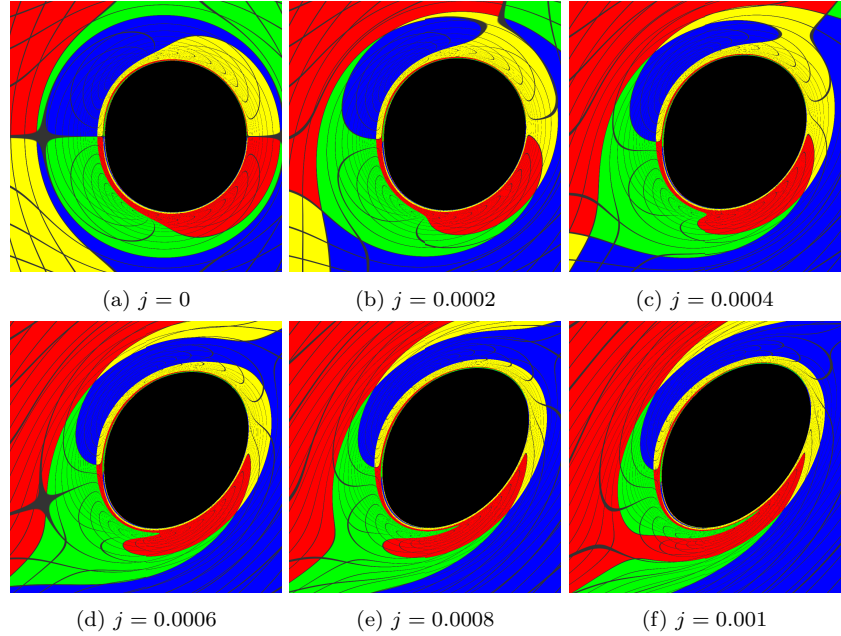


Fig. 5: We show the lensing images for a rapidly rotating KBHSU with $a = 0.9M$ and different values of the swirling parameter j . The observer is set on the equatorial plane at $r_o = 15$.

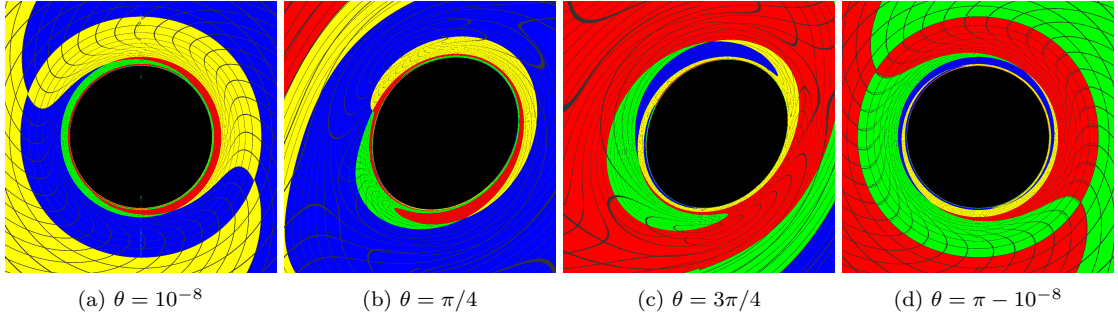


Fig. 6: We show the lensing images for a Kerr swirling spacetime with $a = 0.9M$, $j = 0.0008$ and different observer's angles θ . The observer is set at $r_o = 15$. The lensing image for the observer at $\pi/2$ is given in Fig. 5

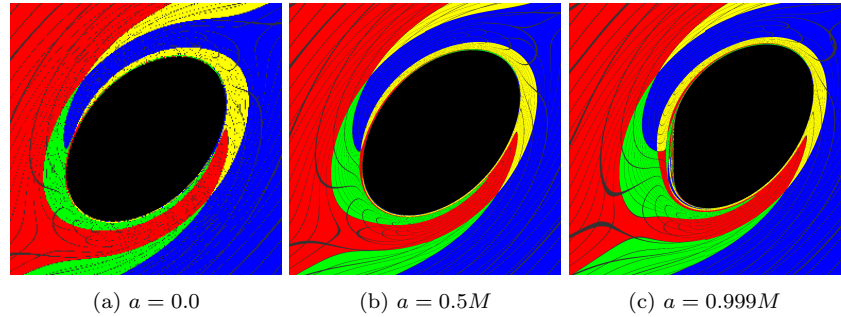


Fig. 7: We show the lensing images for a Schwarzschild/Kerr swirling spacetime with a fixed value of $j = 0.001$ and different values of the angular momentum parameter, a . The observer is set on the equatorial plane at $r_o = 15$, $\theta_o = \pi/2$.

5. CONCLUSIONS

Kerr black holes in a swirling universe are closed form solutions in General Relativity, obtained by well-known transformations from the Kerr black hole seed solution [4]. Unlike the Schwarzschild black holes in a swirling universe, however, the interaction between the black hole spin and the swirling parameter does not yield a (odd) \mathbb{Z}_2 symmetry of the spacetime. Thus the upper and lower hemispheres are not related by a simple symmetry transformation.

Here we have investigated some properties of this spacetime. First we have recalled the conical singularities, which diverge at a critical value of the modulus of the parameter combination $ajM = 0.25$, where both spin parameters enter. Next we have addressed the ergoregions. These also exhibit a notable change in the vicinity of the critical value. Whereas for small ajM , upper and lower hemispheres possess disconnected counter-rotating non-compact ergoregions in addition to the common ergoregion of the Kerr black hole, this changes in the vicinity of the critical value. For larger values of ajM , the three disconnected regions merge to become one infinitely extended ergoregion with hence only one sense of direction.

Then we addressed the first of our main objectives, the light rings in these KBHSU spacetimes. For the SBHSU spacetime the degenerate Schwarzschild LRs split up in a symmetrical way with increasing swirling parameter and move towards the horizon and the poles. For the KBHSH spacetime the picture is far more interesting. In particular, at about the critical value of $ajM = 0.25$ a third LR appears from the axis. But the three LRs co-exist then only in a small range of the spin parameters, until one of the two original LRs disappears. Moreover, in contrast to the SBHSU spacetime, the LRs typically possess different radii.

Finally, we investigated the shadow of KBHSU spacetimes, our second main objective. Since the KBHSU metric is Petrov type I and hence the equations describing geodesic motion are not separable, we had to employ fully numerical methods to obtain the shadows seen by observers outside the black hole. The SBHSU shadows exhibit an odd- \mathbb{Z}_2 symmetry for observers in the equatorial plane. The interaction between the spins of the KBHSU spacetime does not allow for such odd- Z_2 symmetric shadows. All shadows are twisted, though, which would make the appearance of such a black hole most unusual.

While the spacetime may not appear very realistic given the well-known features of our universe, it may still have features that might be of relevance. Here we would like to point out that the universe is threaded by huge structures, cosmic filaments, that rotate and thus might be modelled in part by the swirling universe solutions. Moreover, Astorino et al. [4] considered the swirling universe solutions as possibly relevant in the description of the collision of rotating galaxies. Finally, we would like to mention that it has recently been proposed that a rotating universe might solve the Hubble tension [26].

The KBHSU is also interesting from another point of view : it is an example of a space-time in which test particle motion is chaotic [27]. It would hence be an ideal system to quantify and qualify chaotic behaviour. This could lead to a better understanding of the underlying connection between chaotic test particle motion and the algebraic classification of solutions generated via suitable transformations in the Ernst formalism.

Acknowledgments: R.C. would like to thank CAPES for financial support under Grant No: 88887.371717/2019-00.

[1] K. Gödel: An Example of a New Type of Cosmological Solutions of Einstein's Field Equations of Gravitation, *Rev. Mod. Phys.* **21**, 447 (1949)

[2] A. H. Taub: Empty spacetimes admitting a three parameter group of motions, *Annals Math.* **53**, 472 (1951)

[3] E. Newman, L. Tamburino and T. Unti: Empty space generalization of the Schwarzschild metric, *J. Math. Phys.* **4**, 915 (1963)

[4] M. Astorino, R. Martelli and A. Viganò: Black holes in a swirling universe, *Phys. Rev. D* **106**, 064014 (2022)

[5] G. W. Gibbons, A. H. Moustafa and C. N. Pope: Ergoregions in Magnetised Black Hole Spacetimes, *Class. Quant. Grav.* **30**, 125008 (2013)

[6] R. Capobianco, B. Hartmann and J. Kunz: Geodesic motion in a swirling universe: The complete set of solutions, *Phys. Rev. D* **109**, 064042 (2024)

[7] K. Gjorgjieski and R. Capobianco: Accretion structures around Kerr black holes in a swirling background, *Eur. Phys. J. C* **85**, 597 (2025)

[8] J. Barrientos, A. Cisterna, I. Kolář, K. Müller, M. Oyarzo and K. Pallikaris, *Eur. Phys. J. C* **84**, no.7, 724 (2024) doi:10.1140/epjc/s10052-024-13093-x [arXiv:2401.02924 [gr-qc]].

[9] A. Di Pinto, Charged and Rotating Black Holes in a Melvin-swirling Universe, [arXiv:2407.11270 [gr-qc]] (2024)

[10] A. Di Pinto, S. Klemm and A. Viganò: Kerr-Newman black hole in a Melvin-swirling universe, *JHEP* **06**, 150 (2025)

[11] V. Cardoso, A. S. Miranda, E. Berti, H. Witek and V. T. Zanchin: Geodesic stability, Lyapunov exponents and quasinormal modes, *Phys. Rev. D* **79**, 064016 (2009)

[12] P. V. P. Cunha and C. A. R. Herdeiro: Stationary black holes and light rings, *Phys. Rev. Lett.* **124**, 181101 (2020)

[13] B. R. Iyer, C. V. Vishveshwara and S. V. Dhurandhar: Ultracompact ($R < 3M$) objects in general relativity, *Class. Quantum Grav.* **2**, 219 (1985)

[14] P. Cunha, V.P., E. Berti and C. A. R. Herdeiro: Light-Ring Stability for Ultracompact Objects, *Phys. Rev. Lett.* **119**, 251102 (2017)

[15] V. Cardoso and P. Pani: Living Rev. Rel. **22**, 4 (2019)

[16] Z. S. Moreira, C. A. R. Herdeiro and L. C. B. Crispino: Twisting shadows: Light rings, lensing, and shadows of black holes in swirling universes, *Phys. Rev. D* **109**, 104020 (2024)

[17] J. M. Bardeen, W. H. Press and S. A. Teukolsky: Rotating black holes: Locally nonrotating frames, energy extraction, and scalar synchrotron radiation, *Astrophys. J.* **178**, 347 (1972)

[18] C. M. Claudel, K. S. Virbhadra and G. F. R. Ellis: The Geometry of photon surfaces, *J. Math. Phys.* **42**, 818 (2001)

[19] E. Teo: Spherical Photon Orbits Around a Kerr Black Hole, *Gen. Rel. Grav.* **35**, 1909 (2003)

[20] K. Hioki and K. i. Maeda: Measurement of the Kerr Spin Parameter by Observation of a Compact Object's Shadow, *Phys. Rev. D* **80**, 024042 (2009)

[21] K. Akiyama *et al.* [Event Horizon Telescope], *Astrophys. J. Lett.* **875**, L1 (2019)

[22] K. Akiyama *et al.* [Event Horizon Telescope], *Astrophys. J. Lett.* **930**, L12 (2022)

[23] P. V. P. Cunha, J. Grover, C. Herdeiro, E. Radu, H. Runarsson and A. Wittig: Chaotic lensing around boson stars and Kerr black holes with scalar hair, *Phys. Rev. D* **94**, 104023 (2016)

[24] P. V. P. Cunha, J. Grover, C. Herdeiro, E. Radu, H. Runarsson and A. Wittig, *Phys. Rev. D* **94**, 104023 (2016)

[25] A. Bohn, W. Throwe, F. Hébert, K. Henriksson, D. Bunandar, M. A. Scheel and N. W. Taylor: What does a binary black hole merger look like?, *Class. Quant. Grav.* **32**, 065002 (2015)

[26] B. E. Szigeti, I. Szapudi, I. F. Barna and G. G. Barnaföldi: Can rotation solve the Hubble Puzzle?, *Mon. Not. Roy. Astron. Soc.* **538**, 3038 (2025)

[27] D. Cao, L. Zhang, S. Chen, Q. Pan and J. Jing: Chaotic motion of particles in the spacetime of a Kerr black hole immersed in swirling universes, *Eur. Phys. J. C* **85** (2025) no.1, 28.